JACS
JOURNAL OF THE AMERICAN CHEMICAL SOCIETY

Communication

pubs.acs.org/JACS

Polymer Structure and Conformation Alter the Antigenicity of Virus-like Particle–Polymer Conjugates

Parker W. Lee,[†] Sergey A. Isarov,[†] Jaqueline D. Wallat,[†] Sudheer K. Molugu,[‡] Sourabh Shukla,[§] Jessie E. P. Sun,[†] Jun Zhang,[†] Yi Zheng,[†] Melissa Lucius Dougherty,[∥] Dominik Konkolewicz,[∥] Phoebe L. Stewart,[‡] Nicole F. Steinmetz,[⊥] Michael J. A. Hore,[†] and Jonathan K. Pokorski*[,†]

[†]Department of Macromolecular Science and Engineering, [‡]Department of Pharmacology, [§]Department of Biomedical Engineering, and [⊥]School of Medicine, Case Western Reserve University, Cleveland, Ohio 44106, United States

[∥]Department of Chemistry and Biochemistry, Miami University, Oxford, Ohio 45056, United States

Supporting Information

ABSTRACT: Covalent conjugation of water-soluble polymers to proteins is critical for evading immune surveillance in the field of biopharmaceuticals. The most common and long-standing polymer modification is the attachment of methoxypoly(ethylene glycol) (mPEG), termed PEGylation, which has led to several clinically approved pharmaceuticals. Recent data indicate that brush-type polymers significantly enhance in vitro and in vivo properties. Herein, the polymer conformation of poly(ethylene glycol) is detailed and compared with those of water-soluble polyacrylate and polynorbornene (PNB) when attached to icosahedral virus-like particles. Small-angle neutron scattering reveals vastly different polymer conformations of the multivalent conjugates. Immune recognition of conjugated particles was evaluated versus PEGylated particles, and PNB conjugation demonstrated the most effective shielding from antibody recognition.

Covalent coupling of hydrophilic polymers to the surface of proteins and nanomaterials has been widely utilized to increase circulation half-life and decrease antigenicity.[1a,b] Linear methoxypoly(ethylene glycol) (mPEG) has been the gold standard for protein-based therapies, with 11 mPEG–protein conjugate drugs currently approved by the FDA.[1c] Advances in mPEG modification chemistry (commonly known as PEGylation) have been scarce. Furthermore, since branched mPEG has been repeatedly shown to be more effective at reducing clearance than linear mPEG,[1a,2] it is clear that the polymer architecture plays a large role in dictating the therapeutic efficacy. Few studies have measured the conformation of PEGylated bioconjugates. Previous reports of the conformation of mPEG chains conjugated to proteins showed that the protein and polymer behave as two independent domains with little interaction.[3,4]

Recent data indicate that advanced polymer architectures provide significant advantages in improving protein efficacy in vitro and in vivo.[5] Next-generation polymers for bioconjugation are often synthesized via controlled radical polymerization, typically yielding polymers with brush-type architectures with a variety of potential side chains.[6] A series of recent studies demonstrated that brush polymer architectures, when grafted to enzymatic proteins, imparted greater shielding characteristics and improved activity compared with linear mPEG.[7,8] This "molecular sieving" effect highlights the critical role that polymer conformation plays in improving biomedical properties and provides an impetus to synthesize conjugates with new polymer conformations.

Water-soluble polymers derived from ring-opening metathesis polymerization (ROMP) offer a unique conformational alternative due to the alternating vinyl bonds and ring structures in the backbone of the resulting polynorbornene (PNB) polymers.[9] Small-angle neutron scattering (SANS) studies of mPEG-functionalized PNB indicated that the free polymers adopt a rigid coil conformation distinctly different from the random coil adopted by linear mPEG. Furthermore, proteins conjugated with PNBs are non-cytotoxic.[9c] In view of their biocompatibility, immune-masking properties, and ability to facilitate therapeutic delivery, there is significant motivation to conduct detailed structural studies of PNB bioconjugates.

Virus-like particles (VLPs) are emerging tools for nanomedicine because of their monodispersity, well-defined shapes and sizes, and precise placement of chemical handles for conjugation of drugs, targeting ligands, and polymers.[10a] Noninfectious VLPs have been utilized for tumor targeting, drug delivery, immunotherapy, and imaging,[10b] while gene-delivery vectors have also been extensively researched.[10c] However, since VLPs stimulate innate and humoral immune responses, overcoming immune surveillance remains a challenge. For example, studies using adeno-associated virus have shown that repeat injections limit efficacy and can result in adverse inflammatory immune responses.[10d] These effects can be mitigated by genetic engineering or by covalent coupling of polymers to the capsid surface.[10c,e]

This study describes the conformation of several biocompatible polymers conjugated to VLPs derived from the bacteriophage Qβ, a 28 nm icosahedral virus with a structure known to atomic resolution. Qβ has served as a platform for drug delivery and vaccine development.[11] Qβ conjugates were synthesized using a grafting-to approach with end-functionalized amine-reactive polymers. Qβ–polymer conjugates were prepared with linear mPEG, poly(oligo(ethylene glycol) methyl ether acrylate) (POEGMEA), and anhydride-end-capped poly(norbornene–

Received: November 9, 2016
Published: January 25, 2017

DOI: 10.1021/jacs.6b11643
J. Am. Chem. Soc. 2017, 139, 3312–3315

(oligo(ethylene glycol) ester)) (PNB), each with a target M_n of 10 kDa, corresponding to degrees of polymerization of ~220, ~30, and ~18, respectively (Scheme 1 and Figures S1–S3).[9c,12] A

Scheme 1. Synthesis of Qβ–Polymer Conjugates

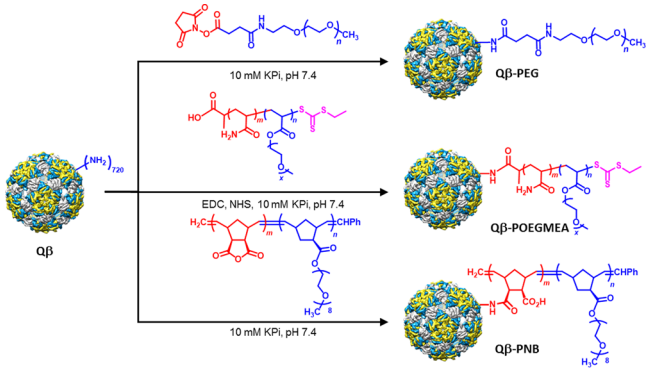

10 kDa target was selected to match that of mPEG in FDA-approved protein–mPEG conjugates (typically 10–12 kDa).[1c] POEGMEA was chosen since similar polymers have shown promise in in vitro and in vivo systems.[8]

Qβ consists of 180 copies of identical capsid proteins, with each capsid protein containing four reactive amines, resulting in 720 amines available for polymer conjugation per particle; however, individual amines show reactivity differences.[13] SDS-PAGE analysis of the conjugates indicated successful polymer attachment (Figures 1A and S4). Pixel density analysis indicated

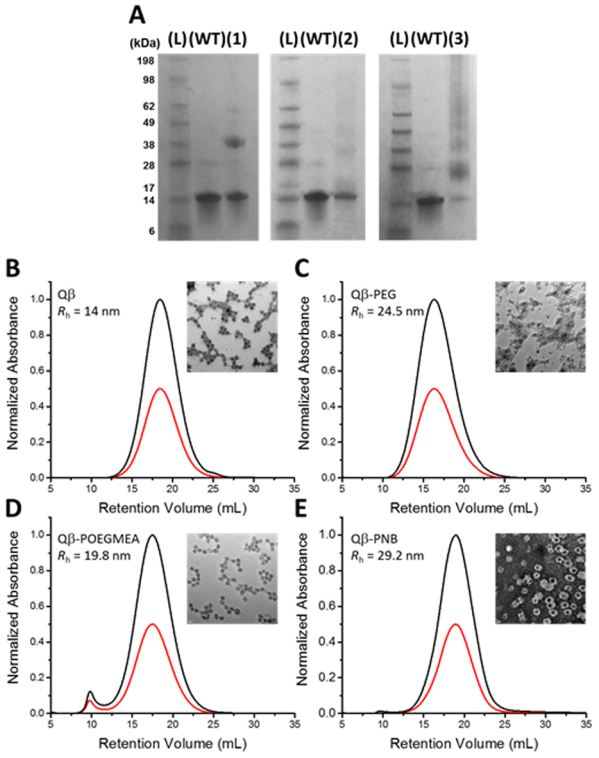

Figure 1. Characterization of Qβ conjugates. (A) SDS-PAGE gel images; L = ladder, WT = unmodified Qβ, 1 = Qβ–PEG, 2 = Qβ–POEGMEA, 3 = Qβ–PNB. (B–E) FPLC chromatograms of particles (black, 260 nm; red, 280 nm) and (insets) TEM micrographs (scale bar = 20 nm) of (B) Qβ, (C) Qβ–PEG, (D) Qβ–POEGMEA, and (E) Qβ–PNB.

Qβ conjugates with ~84, ~ 65, and ~136 chains of mPEG, POEGMEA, and PNB attached per particle, respectively. PAGE gels stained with BaI_2 (specific for PEG) showed bands colocalized with those stained with Coomassie, further confirming conjugation (Figure S5). Grafting-to approaches are typically low-yielding because of steric crowding, resulting in incomplete conjugation. Interestingly, both the POEGMEA and PNB polymers resulted in more di- and trifunctionalized coat proteins, likely as a result of the smaller radius of gyration (R_g) of the polymer (as described in the SANS section) and hence lower steric hindrance during conjugation. Dynamic light scattering (DLS) measurements indicated an increase in hydrodynamic radius of all three conjugates from 14 nm for Qβ to 24.5, 19.8, and 29.2 nm for Qβ–PEG, Qβ–POEGMEA, and Qβ–PNB respectively (Figure S6). The difference in radius between Qβ–POEGMEA and Qβ–PNB is likely due to differences in grafting density, resulting in an increase in polymer shell thickness of the PNB conjugate. Fast protein liquid chromatography (FPLC) was carried out to determine the purity. The elution volumes of Qβ–PEG and Qβ–POEGMEA decreased to 16.3 and 17.4 mL, respectively, relative to Qβ (18.5 mL), indicating an increase in size (Figure 1B–E). A small aggregate peak at 10 mL was observed for Qβ–POEGMEA, likely as a result of intermolecular cross-linking during coupling. Qβ–PNB eluted at 18.9 mL as a single peak. The unexpected change in elution volume is due to interactions between PNB and the chromatography medium, as observed previously.[9c] Transmission electron microscopy (TEM) visualization of the conjugates verified the particle integrity (Figure 1B–E). Of note, TEM micrographs of Qβ–PNB particles revealed an electron-dense coating around individual particles, indicating the presence of tightly compacted polymer on the capsid surface. Neither the mPEG nor POEGMEA polymers could be directly visualized by TEM because the uranyl acetate stain does not interact with PEG.[14]

SANS was used to determine the structures of Qβ, the free polymers, and the Qβ–polymer conjugates in deuterated phosphate buffer (Figures 2 and S7). SANS allows the measurement and separation of signals from proteins and polymers, elucidating their structures and interactions.[4] SANS of Qβ exhibited a clear oscillatory pattern that did not change as the temperature was increased from 25 °C (black squares) to 37 °C (blue circles) (Figure 2A), indicating a stable structure with uniform particle size. The best fit to these data, using a core–shell spherical form factor, indicated a hollow particle with an inner radius of 11.53 ± 0.01 nm and a 1.40 ± 0.02 nm thick shell, in good agreement with the known structure.[15] Interestingly, the small upturn in scattering intensity at low scattering vector (q) implies minor aggregation of Qβ at both temperatures that was not evident from chromatographic analysis and was potentially due to transient hydrophobic interparticle interactions. However, Qβ–PEG showed no such low q upturn, indicating that mPEG conjugation eliminates aggregation and leads to highly dispersed VLPs in solution. SANS of Qβ–PEG was fit with a polymer-grafted core–shell sphere model, which indicated approximately 80 mPEG chains per particle, in good agreement with the PAGE results. The R_g for the Qβ–PEG conjugate was 3.7 nm, which scales with the degree of polymerization (N) as $R_g \sim N^{0.53}$, indicating a slightly swollen polymer conformation. The size and conformation of the PEG chains did not differ in the grafted and free states or with temperature, in agreement with previous mPEG conjugate studies indicating that the polymer and protein behave as two independent domains. Free POEGMEA and PNB exhibited more complex behaviors,

DOI: 10.1021/jacs.6b11643
J. Am. Chem. Soc. 2017, 139, 3312–3315

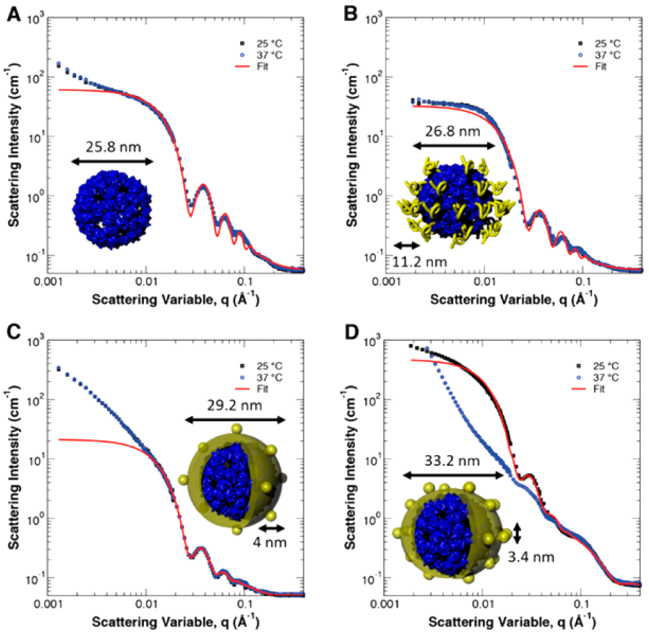

Figure 2. SANS of Qβ–polymer conjugates. Red lines: least-squares fits to the data using either a core–shell model (A), a core–shell chain model (B) or a core–shell raspberry model (C, D). Insets: graphical representations of the fitted models for (A) Qβ, (B) Qβ–PEG, (C) Qβ–POEGMEA, and (D) Qβ–PNB.

adopting collapsed globular conformations in solution. Fits to free POEGMEA and PNB found R_g = 2.12 and 2.16 nm, respectively, with a size that scaled roughly as $R_g \sim N^{0.25}$, indicating a dense globular conformation. On the basis of the observed conformations of the free polymers, Qβ–POEGMEA and Qβ–PNB were modeled as hollow capsules decorated with spherical polymer domains (i.e., "hollow raspberries"). Fits to the SANS data for Qβ–POEGMEA (Figure 2C) indicated that the inner radius of the particle remained unchanged and that the particle was grafted with 26 polymer globules, each with an average radius of 2 nm. Interestingly, the shell thickness increased from 1.4 nm for wild-type Qβ to 3.6 nm for Qβ–POEGMEA, implying that, in addition to the globules, the polymer formed a surface layer of 2.2 nm. The number of globules determined via SANS is lower than that of grafted chains determined via PAGE, likely because not all of the polymer chains form globules and globules may form from multiple chains, especially given the increase in the particle shell thickness. While the SANS data do not display a temperature dependence, substantial aggregation of Qβ–POEGMEA is indicated by a large upturn in the low-q scattering intensity.

The solution structure of Qβ–PNB particles is similar to that of Qβ–POEGMEA but displays a temperature-dependent behavior. Fits to SANS measurements using a hollow raspberry model (Figure 2D) found that 127 PNB globules were grafted to the surface, with an average radius of 1.7 nm per globule. The Qβ–PNB particles exhibited a polymer shell with a thickness of 4.2 nm, which is considerably larger than that in Qβ–POEGMEA, likely as a result of the increased density of PNB chains on the capsid. The small upturn in scattering intensity at low q (25 °C) indicates a small amount of aggregation in the system. At 37 °C significant aggregation and phase separation of the particles from solution was observed, as indicated by the large power law at low q and a reduction in scattering peak intensity. This is noteworthy since the lower critical solution temperature (LCST) of the free polymer was reported to be 70 °C, showing that multivalency is critical in determining the interaction parameters.[16] The LCST behavior was further studied by turbidity measurements and observed only at concentrations above 5 mg mL^{-1} (Figure S8). However, given the similarity between the data at high q (i.e., $q > 0.1$ Å^{-1}), it is unlikely that the polymer conformation changes significantly. These SANS results indicate that POEGMEA and PNB adopt distinctly different conformations than linear PEG.

Cryo-EM studies of Qβ and Qβ–PNB enabled direct visualization of the grafted PNB (Figure S9). The alternative formulations were excluded, since no polymer electron density was visible in negative-stained micrographs. The cryo-micrograph of Qβ shows ~30 nm diameter icosahedral particles, as expected (Figure S9A), while that of Qβ–PNB shows particles with fuzzy halos (Figure S9B). Single-particle reconstruction of the Qβ particle images using the RELION software package[17] produced a highly ordered capsid at 4.5 Å resolution (Figure 3A,B), in good agreement with the crystal structure (Figure S10).[16] Reconstruction of Qβ–PNB was complicated by the presence of the heterogeneous polymer layer surrounding the capsid. However, limited refinement with the EMAN software package[18] produced a structure with moderate resolution (~15 Å) (Figure 3C,D). The resolutions of both structures were analyzed by ResMap (Figure S11).[19] This structure reveals polymer density covering most of the capsid and extending ~2.5 nm from the viral surface with additional heterogeneous polymeric extensions reaching out to ~15 nm from the viral surface. These findings correlate well with the DLS and SANS studies, indicating a polymer shell interacting with the capsid as well as polymer extensions dispersed around the shell.

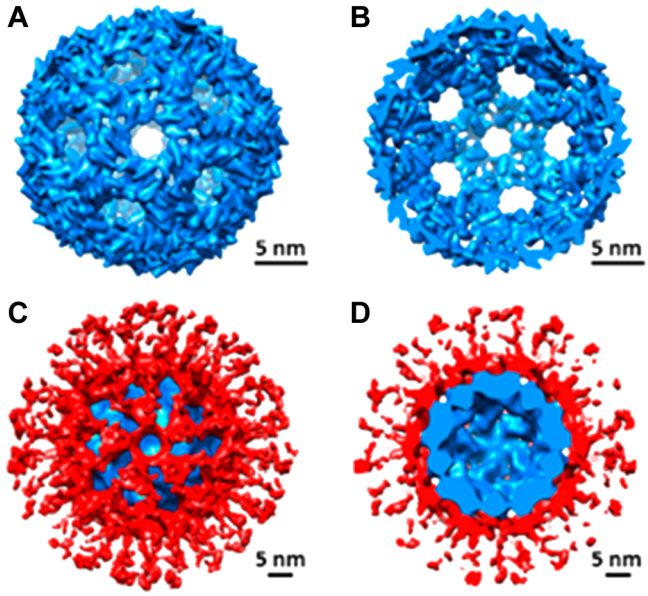

Figure 3. Cryo-EM reconstructions of Qβ and Qβ–PNB. (A) Surface representation of the Qβ structure filtered to 15 Å resolution. (B) Cropped representation revealing the internal cavity of Qβ. (C) Surface representation of Qβ–PNB: blue, virion density; red, polymer. (D) Cropped representation revealing the internal cavity of Qβ–PNB.

To assess whether the different polymers would enable evasion of carrier-specific antibodies, the sera of mice immunized with Qβ were assayed for recognition of "naked" Qβ versus the polymer-coated particle formulations (Figure S12). Relative to

DOI: 10.1021/jacs.6b11643
J. Am. Chem. Soc. 2017, 139, 3312–3315

unmodified Qβ, POEGMEA coating reduced the antibody recognition by 16% while the mPEG and PNB coatings reduced the antigenicity by 42% and 49%, respectively (Figure 4). This is

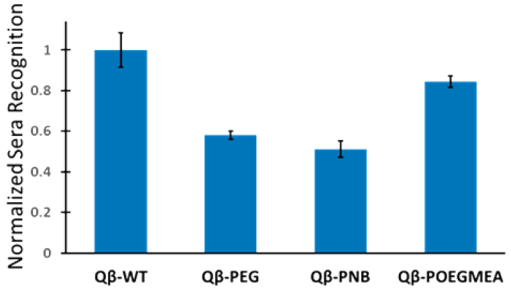

Figure 4. ELISA response using Qβ-immunized sera (n = 4) for detection of polymer conjugates. Results are normalized to recognition of unmodified Qβ.

noteworthy since 10 kDa PNB occupies approximately one-third of the hydrodynamic volume of 10 kDa PEG. The effectiveness of antibody shielding of Qβ−PEG and Qβ−PNB points to two different mechanisms of evasion. The PNB shell likely prevents anti-Qβ immunoglobulin G (IgG) from reaching the capsid and diminishes antibody binding. In contrast, Qβ−POEGMEA, while having a similar polymer conformation as Qβ−PNB, only has a modest effect in reducing antibody recognition. POEGMEA forms a thinner shell on the surface of Qβ and fewer polymer globules relative to PNB. This implies that the method of polymer conjugation is extremely important, since the shell thickness is likely correlated to the grafting density. The polymers used were conjugated such that the maximum grafting density for each species was achieved. However, EDC coupling significantly diminished the coupling efficiency for POEGMEA, which likely played a role in the anti-Qβ IgG recognition of the surface. In part, the high coupling efficiency of PNB contributed to the stealth properties of the polymer. Taken together, these results clearly demonstrate that interactions between the polymer and protein components can critically alter immune recognition.

The results of this study indicate that Qβ−PNB conjugates have a unique surface polymer conformation compared with Qβ conjugated to mPEG, as determined via SANS and cryo-EM. Relative to mPEG and POEGMEA, PNB affords greater antibody shielding to the conjugate while occupying a significantly smaller hydrodynamic volume. Investigation of the structure and conformation of polymer-grafted VNPs and correlation with immune evasion provides valuable information for the development of next-generation VNP−polymer conjugates.

■ ASSOCIATED CONTENT

Supporting Information

The Supporting Information is available free of charge on the ACS Publications website at DOI: 10.1021/jacs.6b11643.

Procedures and additional data (PDF)

■ AUTHOR INFORMATION

Corresponding Author

*jon.pokorski@case.edu

ORCID

Dominik Konkolewicz: 0000-0002-3828-5481

Michael J. A. Hore: 0000-0003-2571-2111

Jonathan K. Pokorski: 0000-0001-5869-6942

Notes

The authors declare no competing financial interest.

■ ACKNOWLEDGMENTS

We acknowledge NIST for providing the neutron research facilities used, supported in part by NSF (DMR-1508249). This work was funded in part through Grants NIH-R21HL121130 (N.F.S.) and NSF-CHE1306447 (J.K.P., N.F.S.). We acknowledge CWRU's high-performance computing cluster.

■ REFERENCES

(1) (a) Lee, K. L.; Shukla, S.; Wu, M.; Ayat, N. R.; El Sanadi, C. E.; Wen, A. M.; Edelbrock, J. F.; Pokorski, J. K.; Commandeur, U.; Dubyak, G. R.; Steinmetz, N. F. *Acta Biomater.* **2015**, *19*, 166. (b) Bruckman, M. A.; Randolph, L. N.; VanMeter, A.; Hern, S.; Shoffstall, A. J.; Taurog, R. E.; Steinmetz, N. F. *Virology* **2014**, *449*, 163. (c) Alconcel, S. N. S.; Baas, A. S.; Maynard, H. D. *Polym. Chem.* **2011**, *2*, 1442.

(2) Bailon, P.; Palleroni, A.; Schaffer, C. A.; Spence, C. L.; Fung, W. J.; Porter, J. E.; Ehrlich, G. K.; Pan, W.; Xu, Z. X.; Modi, M. W.; Farid, A.; Berthold, W.; Graves, M. *Bioconjugate Chem.* **2001**, *12*, 195.

(3) He, L.; Wang, H.; Garamus, V. M.; Hanley, T.; Lensch, M.; Gabius, H.-J.; Fee, C. J.; Middelberg, A. *Biomacromolecules* **2010**, *11*, 3504.

(4) Pai, S. S.; Hammouda, B.; Hong, K.; Pozzo, D. C.; Przybycien, T. M.; Tilton, R. D. *Bioconjugate Chem.* **2011**, *22*, 2317.

(5) (a) Nguyen, T. H.; Kim, S.-H.; Decker, C. G.; Wong, D. Y.; Loo, J. A.; Maynard, H. D. *Nat. Chem.* **2013**, *5*, 221. (b) Fuhrmann, G.; Grotzky, A.; Lukić, R.; Matoori, S.; Luciani, P.; Yu, H.; Zhang, B.; Walde, P.; Schlüter, A. D.; Gauthier, M. A.; Leroux, J.-C. *Nat. Chem.* **2013**, *5*, 582.

(6) (a) Wallat, J. D.; Rose, K. A.; Pokorski, J. K. *Polym. Chem.* **2014**, *5*, 1545. (b) Averick, S.; Mehl, R. A.; Das, S. R.; Matyjaszewski, K. *J. Controlled Release* **2015**, *205*, 45.

(7) Liu, M.; Tirino, P.; Radivojevic, M.; Phillips, D. J.; Gibson, M. I.; Leroux, J.-C.; Gauthier, M. A. *Adv. Funct. Mater.* **2013**, *23*, 2007.

(8) Liu, M.; Johansen, P.; Zabel, F.; Leroux, J.-C.; Gauthier, M. A. *Nat. Commun.* **2014**, *5*, 5526.

(9) (a) Kammeyer, J. K.; Blum, A. P.; Adamiak, L.; Hahn, M. E.; Gianneschi, N. C. *Polym. Chem.* **2013**, *4*, 3929. (b) Miki, K.; Oride, K.; Inoue, S.; Kuramochi, Y.; Nayak, R. R.; Matsuoka, H.; Harada, H.; Hiraoka, M.; Ohe, K. *Biomaterials* **2010**, *31*, 934. (c) Isarov, S. A.; Lee, P. W.; Pokorski, J. K. *Biomacromolecules* **2016**, *17*, 641.

(10) (a) Chen, Z.; Li, N.; Li, S.; Dharmarwardana, M.; Schlimme, A.; Gassensmith, J. J. *WIREs. Nanomed. Nanobiotechnol.* **2016**, *8*, 512. (b) Pokorski, J. K.; Steinmetz, N. F. *Mol. Pharmaceutics* **2011**, *8*, 29. (c) Gonçalves, M. A. *Virol. J.* **2005**, *2*, 43. (d) Sun, J. Y.; Anand-Jawa, V.; Chatterjee, S.; Wong, K. K. *Gene Ther.* **2003**, *10*, 964. (e) Le, H. T.; Yu, Q.-C.; Wilson, J. M.; Croyle, M. A. *J. Controlled Release* **2005**, *108*, 161.

(11) (a) Pokorski, J. K.; Breitenkamp, K.; Liepold, L. O.; Qazi, S.; Finn, M. G. *J. Am. Chem. Soc.* **2011**, *133*, 9242. (b) Spohn, G.; Keller, I.; Beck, M.; Grest, P.; Jennings, G. T.; Bachmann, M. F. *Eur. J. Immunol.* **2008**, *38*, 877.

(12) Falatach, R.; McGlone, C.; Al-Abdul-Wahid, M. S.; Averick, S.; Page, R. C.; Berberich, J. A.; Konkolewicz, D. *Chem. Commun.* **2015**, *51*, 5343.

(13) Astronomo, R. D.; Kaltgrad, E.; Udit, A. K.; Wang, S.-K.; Doores, K. J.; Huang, C.-Y.; Pantophlet, R.; Paulson, J. C.; Wong, C.-H.; Finn, M. G.; Burton, D. R. *Chem. Biol.* **2010**, *17*, 357.

(14) De Carlo, S.; Harris, J. R. *Micron* **2011**, *42*, 117.

(15) Golmohammadi, R.; Fridborg, K.; Bundule, M.; Valegård, K.; Liljas, L. *Structure* **1996**, *4*, 543.

(16) Cheng, G.; Hua, F.; Melnichenko, Y. B.; Hong, K.; Mays, J. W.; Hammouda, B.; Wignall, G. D. *Eur. Polym. J.* **2008**, *44*, 2859.

(17) Scheres, S. H. W. *J. Struct. Biol.* **2012**, *180*, 519.

(18) Ludtke, S. J.; Baldwin, P. R.; Chiu, W. *J. Struct. Biol.* **1999**, *128*, 82.

(19) Swint-Kruse, L.; Brown, C. S. *Bioinformatics* **2005**, *21*, 3327.

DOI: 10.1021/jacs.6b11643
J. Am. Chem. Soc. 2017, 139, 3312−3315